CHEMISTRY OF MATERIALS
Article

Chem. Mater. **2010,** *22,* 5383–5391 5383
DOI:10.1021/cm1018508

Reactive Silver and Cobalt Nanoparticles Modified with Fatty Acid Ligands Functionalized by Imidazole Derivatives

Lev Bromberg, Liang Chen, Emily P. Chang, Sa Wang, and T. Alan Hatton*

Department of Chemical Engineering, Massachusetts Institute of Technology, Cambridge, Massachusetts 02139

Received July 2, 2010. Revised Manuscript Received August 6, 2010

Novel nucleophilic ligands were synthesized from oleic acid conjugated with 2-mercaptoimidazole via a UV-initiated thiol−ene reaction, and by a condensation of *trans*-9,10-epoxystearic acid with 4(5)-imidazoledithiocarboxylic acid. Nanoparticles (NPs) with 10−100 nm Ag(0) or Co(0) cores were obtained by reduction of Ag^+ or Co^{2+} by borohydride in *N*,*N*-dimethylformamide or aqueous solutions respectively. The NPs capped with oleic acid or 9,10-epoxystearic acids were further covalently bound to 2-mercaptoimidazole or 4(5)-imidazoledithiocarboxylic acid. The ligands and NPs functionalized with nucleophilic imidazole moieties enabled facile hydrolysis of paraoxon (O,O-diethyl O-(*p*-nitrophenyl) phosphate) by NPs in their aqueous media. The NPs acted as recoverable semiheterogeneous catalysts. The paraoxon hydrolysis was accelerated 10- to 50-fold by the formation of complexes between the imidazole-containing ligands or NPs with Co^{2+}.

Introduction

Transition metal and metal oxide nanoparticles have generated significant interest because of their large surface-to-volume ratios, functional properties, and important applications, ranging from electronics and catalysis to biomedicine.[1,2] Our specific area of interest has been nanoparticles (NPs) with a metal or metal oxide core that is functionalized with an organic ligand, either a small-molecular-weight species or a polymer, tailored for the destruction of toxins.[3−5] Our NP design is based on the reactivity of the ligand, and not on the catalytic properties of a transition metal per se. The core of the ligand-decorated NP is nonreactive, but determines the NP shape and size, while facilitating the particle recoverability. The NPs can be readily recovered from the reaction medium by centrifugation or filtration. Large surface area, small thickness (up to 10% of the total hydrodynamic diameter of a given NP) and compatibility of the ligand shell with the continuous phases ensure accessibility of the reactive ligands to the reagents.

Our catalytic NP is a hybrid between the supported transition metal particles and functional polymeric colloids. Because of the multifunctionality of the organic ligands, our NPs are not only capable of carrying out catalytic functions but can also bind strongly to bacterial membranes and kill various germs, thus acting as efficient disinfectants.[6,7] Previously, the majority of the ligands we employed to impart esterolytic function to the NP and other colloids have been oximes, hydroxamic acids, iodosobenzoates, and other α-nucleophiles.[3,4,8,9] Although capable of facile hydrolysis of organophosphorous (OP) pesticides and chemical warfare agents, α-nucleophiles are quite sensitive to the presence of compounds that are not targeted and can also undergo transformations rendering them unreactive, such as Beckmann and Lossen rearrangements. Therefore, in the present work, our goal was to create NPs functionalized with imidazole derivatives.

Polymers and nanosized assemblies functionalized with imidazole catalyze esterolytic and proteolytic reactions.[10−19]

*Corresponding author. E-mail: tahatton@mit.edu.

(1) Fedlheim, D. L. ; Foss, C. A. *Metal Nanoparticles: Synthesis, Characterization, and Applications*; CRC Press: Boca Raton, FL, 2001; 352 pp.
(2) Rotello, V. *Nanoparticles: Building Blocks for Nanotechnology*; Springer: New York, 2004. *Nanoparticles and Catalysis*; Astruc, D., Ed.; Wiley-VCH: Weinheim, Germany, 2008.
(3) Bromberg, L.; Hatton, T. A. *Ind. Eng. Chem. Res.* **2005**, *44*, 7991–7998.
(4) Bromberg, L.; Hatton, T. A. *Ind. Eng. Chem. Res.* **2007**, *46*, 3296–3303.
(5) Hatton; T. A., Bromberg; L. E. Catalytic nanoparticles for nerve-agent destruction. U.S. Patent 7 598 199, October 6, 2009.
(6) Bromberg, L.; Raduyk, S.; Hatton, T. A. *Anal. Chem.* **2009**, *81*, 5637–5645.
(7) Bromberg, L.; Chang, E. P.; Alvarez-Lorenzo, C.; Magarinos, B.; Concheiro, A.; Hatton, T. A. *Langmuir* **2010**, *26*, 8829–8835.
(8) Bromberg, L.; Zhang, H.; Hatton, T. A. *Chem. Mater.* **2008**, *20*, 2001–2008.
(9) Bromberg, L.; Schreuder-Gibson, H.; Creasy, W. R.; McGarvey, D. J.; Fry, R. A.; Hatton, T. A. *Ind. Eng. Chem. Res.* **2009**, *48*, 1650–1659.
(10) Overberger, C. G.; Salamone, J. C. *Acc. Chem. Res.* **1969**, *2*, 217–224.
(11) Overberger, C. G.; Kwon, B.-D. In *Initiation of Polymerization*; Bailey, F. E., Jr., Vandeberg, E. J., Blumstein,A., Bowden, M. J., Arthur, J. C., Lal, J., Ottenbrite, R. M., Eds.; ACS Symposium Series; American Chemical Society: Washington, D.C., 1983; Vol. *212*, Chapter 6, pp 65−74.
(12) Overberger, C. G.; Tomko, R. In *Initiation of Polymerization*; Bailey, F. E., Jr., Vandeberg, E. J., Blumstein,A., Bowden, M. J., Arthur, J. C., Lal, J., Ottenbrite, R. M., Eds.; ACS Symposium Series; American Chemical Society: Washington, D.C., 1983; Vol. *212*, Chapter 2, pp 13−21.
(13) Guler, M. O.; Stupp, S. I. *J. Am. Chem. Soc.* **2007**, *129*, 12082–12083.
(14) Kitano, H.; Sun, Z.; Ise, N. *Macromolecules* **1983**, *16*, 1823–1827.

Published on Web 08/20/2010

The mechanism of the ester hydrolysis catalysis by low-molecular-weight imidazole derivatives is a function of the ester (substrate) structure.[20−26] Esters that possess poor leaving groups are subject to classical general base catalysis by imidazole, whereas esters with good leaving groups are subject to nucleophilic catalysis.[20] In polymers and colloidal assemblies, the activity of the imidazole group (much like in enzymes), depends on its microenvironment such as the presence of hydrophobic or hydrophilic moieties, as well as other imidazole groups, in its proximity.[19] In that regard, we were interested in potential neighboring effects of the imidazole groups concentrated in the organic shell, on esterolytic reactions. It has been shown that self-assembling monolayers of various ligands form a multitude of patterns on the NP surfaces, which affect the microenvironment of the ligands and hence the NP solvation and its interaction with substrates.[27] The confinement of the catalytic units to the monolayer covering the NP triggers a cooperative, pH-dependent hydrolytic mechanism in which an imidazolium ion acts as a catalyst.[28−30]

Noting the widespread use of fatty acids as steric and electrostatic stabilizers for the colloidal stability of NPs,[31,32] in the present work, we created functional fatty acid-imidazole conjugates for the NP surface modification. Because oleic acid is strongly surface-active and possesses a reactive unsaturated bond, we concentrated on its use for conjugating with imidazole derivatives, along with its epoxidized derivative, *trans*-9,10-epoxystearic acid. Thiol−ene coupling reactions involving the double bond of oleic acid and its esters are known.[33] Commercially available derivatives of imidazole such as 2-mercaptoimidazole and 4(5)-imidazoledithiocarboxylic acid were chosen for conjugation with oleic acid and its derivative. 2-Mercaptoimidazole is a reactive, neutral nucleophile (pK_a of the thiol group ionization, 11.6)[34,35] capable of participating in thiol−ene reactions,[35,36] which are facilitated by the relatively low S−H bond dissociation energy, and even more readily, in conjugation reactions with epoxy groups.[37] 2-Mercaptoimidazole is also a bioactive metal-complexing agent.[38−43] Likewise, the reactivity of the dithio group and metal-chelating capability of the dithio and imidazole functionalities in 4(5)-imidazoledithiocarboxylic acid have made it a building block for synthesis of various metal−organic compounds, functional polymers, and metal ion adsorbents.[44−48]

Testing of the hydrolytic activity of the ligands and nanoparticles was performed using the insecticide paraoxon as a substrate. Hydrolysis of paraoxon and analogous OP pesticides catalyzed by metal ions,[49] micelles of nucleophilic surfactants, and metallomicelles[50−52] and enzymes[53,54] has been studied in detail and such hydrolysis represents a convenient reaction reflecting upon the activity of the catalytic agent used. Although the hydrolysis of paraoxon is of practical importance in its own right from an environmental standpoint,[49] it can also serve as a mechanistic model of degradation of more toxic warfare agents. We chose cobalt and silver to be the cores of our NPs, as their synthesis and detection are well-established,[55,56] yet fatty acids are capable of binding

(15) Overberger, C. G.; Morimoto, M. *J. Am. Chem. Soc.* **1971**, *93*, 3222–3228.
(16) Kitano, H.; Sun, Z. H.; Isa, N. *Macromolecules* **1983**, *16*, 1306–1310.
(17) Kunitake, T.; Shinkai, S. *J. Am. Chem. Soc.* **1971**, *93*, 4256–4263.
(18) Kunitake, T.; Shimada, F.; Aso, C. *J. Am. Chem. Soc.* **1969**, *91*, 2716–2723.
(19) Suh, J.; Oh, S. *J. Org. Chem.* **2000**, *65*, 7534–7540.
(20) Kirsch, J. F.; Jencks, W. P. *J. Am. Chem. Soc.* **1964**, *86*, 837.
(21) Rogers, G. A.; Bruice, B. C. *J. Am. Chem. Soc.* **1974**, *96*, 2463–2473.
(22) Pollack, R. M.; Dumsha, T. C. *J. Am. Chem. Soc.* **1975**, *97*, 377.
(23) Kunitake, T.; Ihara, H.; Okahata, Y. *J. Am. Chem. Soc.* **1983**, *105*, 6070.
(24) Mallick, I. M.; D'Souza, V. T.; Yamaguchi, M.; Lee, T.; Chalabi, P.; Gadwood, R. C.; Bencer, M. L. *J. Am. Chem. Soc.* **1984**, *106*, 7252.
(25) Ohkubo, K.; Uranbe, K.; Yamamoto, J.; Sagawa, T.; Usui, S. J. Chem. Soc., Perkin Tran. 11995, 2957.
(26) Broo, K. S.; Nilsson, H.; Flodberg, A.; Baltzer, L. *J. Am. Chem. Soc.* **1998**, *120*, 4063.
(27) Centrone, A.; Penzo, E.; Sharma, M.; Myerson, J. W.; Jackson, A. M.; Marzari, N.; Stellacci, F. *Proc. Natl. Acad. Sci. U.S.A.* **2008**, *105*(29), 9886–9891.
(28) Lucarini, M.; Franchi, P.; Pedulli, G. F.; Pengo, P.; Scrimin, P.; Pasquato, L. *J. Am. Chem. Soc.* **2004**, *126*, 9326–9329.
(29) Pasquato, L.; Rancan, F.; Scrimin, P.; Mancin, F.; Frigeri, C. *Chem. Commun.* **2000**, 2253–2254.
(30) Pengo, P.; Polizzi, S.; Pasquato, L.; Scrimin, P. *J. Am. Chem. Soc.* **2005**, *127*, 1616–1617.
(31) Yin, Y.; Alivisatos, A. P. *Nature* **2004**, *437*, 664–670.
(32) Harada, T.; Hatton, T. A. *Langmuir* **2009**, *25*, 6407–6412.
(33) Samuelsson, J.; Jonsson, M.; Brinck, T.; Johansson, M. J. *Polym. Sci., Part A: Polym. Chem.* **2004**, *42*, 6346–6352.
(34) Stanovnik, B.; Tisler, M. *Anal. Biochem.* **1964**, *9*, 68–74.
(35) Carlsson, J.; Kierstan, M. P. J.; Brocklienhurst, K. *Biochem. J.* **1974**, *139*, 221–235.
(36) Persson, J. C.; Jannasch, P. *Macromolecules* **2005**, *38*, 3283–3289.
(37) Schwarz, A.; Wilchek, M. U.S. Patent 5 719 269, February 17, 1998.
(38) Tweit, R. C.; Kreider, E. M.; Muir, R. D. *J. Med. Chem.* **1973**, *16*, 1161–1169.
(39) Roser, K. S.; Brookes, P. S.; Wojtovich, A. P.; Olson, L. P.; Shojaie, J.; Parton, R. L.; Anders, M. W. *Bioorg. Med. Chem.* **2010**, *18*, 1441–1448.
(40) Van Lommen, G.; Doyon, J.; Coesemans, E.; Boeckx, S.; Cools, M.; Buntinx, M.; Hermans, B.; VanWauwe, J. *Bioorg. Med. Chem. Lett.* **2005**, *15*, 497–500.
(41) Álvarez-Bustamante, R.; Negrón-Silva, G.; Abreu-Quijano, M.; Herrera-Hernández, H.; Romero-Romo, M.; Cuán, A.; Palomar-Pardavé, M. *Electrochim. Acta* **2009**, *54*(30), 5393–5399.
(42) Ryan, N. T.; Richert, D. A.; Westerfeld, W. W.; Fujishima, M.; Matsuo, Y.; Takatori, H.; Uchida, K. *Electrochem. Commun.* **2008**, *10*, 1482–1485.
(43) Dias Filho, N. L.; Gushikem, Y. *Sep. Sci. Technol.* **1997**, *32*, 2535–2545.
(44) Sawa, N., Saeki, T. Imidazole 4(5)-dithiocarboxylic acids or salts, U.S. Patent 4 394 511, Jul 19, 1983.
(45) Ma, C.; Han, Y.; Zhang, R. *Inorg. Chim. Acta* **2005**, *358*, 3084–3092.
(46) Carter, S.; Hunt, B.; Rimmer, S. *Macromolecules* **2005**, *38*, 4595–4603.
(47) Carter, S.; Rimmer, S.; Rutkaite, R.; Swanson, L.; Fairclough, J. P. A. *Biomacromolecules* **2006**, *7*, 1124–1130.
(48) Grigoropoulou, G.; Stathi, P.; Karakassides, M. A.; Louloudi, M.; Deligiannakis, Y. *Colloids Surf., A: Physicochem. Eng. Aspects* **2008**, *320*, 25–35.
(49) Smolen, J. M; Stone, A. T. *Environ. Sci. Technol.* **1997**, *31*, 1664–1673.
(50) Moss, R. A.; Kanamathareddy, S.; Vijayaraghavan, S. *Langmuir* **2001**, *17*, 6108–6111.
(51) Morales-Rojas, H.; Moss, R. A. *Chem. Rev.* **2002**, *102*, 2497–2522.
(52) Fubin, J.; Fubin, J.; Bingying, J.; Bingying, J.; Xiaoqi, Y.; Xiancheng, Z. *Langmuir* **2002**, *18*, 6769–6774.
(53) Lei, Y.; Mulchandani, A.; Chen, W. *Biotechnol. Prog.* **2005**, *21*, 678–681.
(54) Richter, R. J.; Jarvik, G. P.; Furlong, C. E. *Toxicol. Appl. Pharmacol.* **2009**, *235*, 1–9.
(55) Mulfinger, L.; Solomon, S. D.; Bahadory, M.; Jeyarajasingam, A. V.; Rutkowsky, S. A.; Boritz, C. *J. Chem. Educ.* **2007**, *84*, 322.
(56) Puntes, V. F.; Krishnan, K. M.; Alivisatos, A. P. *Science* **2001**, *291* (5511), 2115–2117.

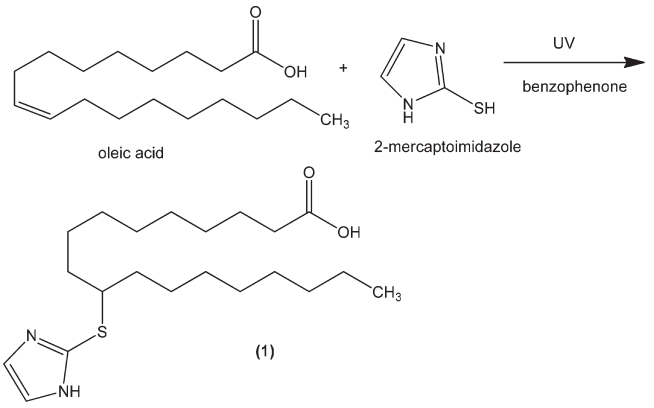

Figure 1. Synthesis of oleic acid and 2-mercaptoimidazole conjugate (**1**) by thiol−ene reaction.

through their carboxylic groups with the surfaces of these metals. On the basis of the above-described rationale, in the present work we designed and synthesized water-dispersible NPs with silver or cobalt cores functionalized by shells of fatty acids modified with imidazole derivatives. The NPs are reactive toward paraoxon, especially in the presence of cobalt(II) ions, as described below.

Experimental Section

Materials. 2-Mercaptoimidazole (98%), *trans*-9,10-epoxystearic acid (99% by TLC), 4(5)-imidazoledithiocarboxylic acid (70%), oleic acid (≥99%), (4-(2-hydroxyethyl)-1-piperazineethanesulfonic acid) (HEPES, 99%), paraoxon-ethyl (*O*,*O*-diethyl *O*-(4-nitrophenyl) phosphate, 98%), cobalt(II) chloride hexahydrate (98%), and silver nitrate (99%) were all obtained from Sigma-Aldrich Chemical Co. and used as received. All other chemicals and solvents were obtained from commercial sources and were of the highest purity available.

Syntheses. *Conjugate of Oleic Acid and 2-Mercaptoimidazole* (*10-((1H-Imidazol-2-yl)thio)octadecanoic acid*) (***1***) (*Figure 1*). A solution of oleic acid (1.0 g, 3.54 mmol), 2-mercaptoimidazole (0.354 g, 3.54 mmol), and benzophenone (50 mg, 0.27 mmol) in 10 mL dry methanol was deaerated and placed in a glass vial, which was subsequently sealed and irradiated using a UV−vis 5000EC flood lamp (spectral output, 300−500 nm; maximum intensity, 250 mW/cm^2 at 365 nm; Dymax Corp, Torrington, CT) for 10 min. The resulting yellow solution was equilibrated at ambient temperature and vacuum-evaporated. The products were separated by TLC (silica gel, aluminum oxide sheets Si 60 F_{254}, 5 × 10 cm, EMD Chemicals, Gibbstown, NJ) using hexane-ethyl acetate (80:20 v/v).[57,58] Yield, 75%. The initial compounds moved with the solvent front; the product observed under UV ($R_f \approx 0.5$) was separated and dissolved in 250 μL of CD_3OD. ^{1}H NMR (CD_3OD, 400 MHz, see the Supporting Information, S1), δ (ppm): 6.8 (2H, imidazole), 3.2 (1H, methine, α to C−S), 2.3 (2H, methylene, α to COOH), 1.55 (2H, methylene), 1.1−1.3 (22H, methylene), 0.87 (3H, methyl). Found (calcd): C, 65.1 (64.82); H, 9.26 (10.34); N, 6.93 (7.56); S, 8.29 (8.65). The solubility of compound **1** was tested at room temperature and at 2.5 mM concentration level. Compound **1** formed clear solutions in water at pH > 5, methanol, ethanol, DMF, and DMSO.

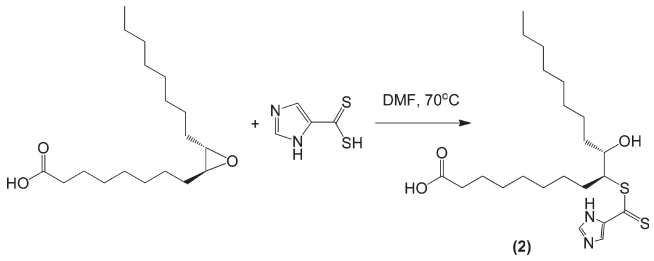

Figure 2. Synthesis of conjugate of *trans*-9,10-epoxystearic and 4(5)-imidazoledithiocarboxylic acids (**2**).

Conjugate of trans-9,10-Epoxystearic and Imidazoledithiocarboxylic Acids (*(9s,10s)-1,1,10-Trihydroxyoctadecan-9-Yl 1H-Imidazole-5-carbodithioate*) (***2***) (*Figure 2*). *trans*-9,10-Epoxystearic acid (30 mg, 0.1 mmol) and 4(5)-imidazoledithiocarboxylic acid (15 mg, 0.1 mmol) were dissolved in 1 mL of *N*,*N*-dimethylformamide and the reaction was conducted in a sealed vial at 70 °C for 24 h. The initial reaction solution was dark-red and became brown at the end of the reaction. The products were purified as follows. The reaction mixture was allowed to cool to ambient temperature and excess deionized water (15 mL) was added. Dark-brown precipitates were formed. The precipitates were centrifuged (12 900 *g*, 15 min) and separated. The solids were redissolved in cold acetone (4 °C, 15 mL). Upon heating to 70 °C, dark-red precipitates were formed in the acetone. The solids were separated from the hot acetone by centrifugation and residual solvent was evaporated under vacuum. Yield, 83%. The TLC in ethanol/acetone (1:1) mixture showed one product ($R_f \approx 0.5$). ^{1}H NMR (DMF-d_7, 400 MHz, S2), δ (ppm): 12.9 (1H, imidazole), 12.1 (1H, H−O−C(=O)), 7.88 (1H, imidazole), 3.48 (1H, methane), 2.24, 151 (2H, methylene), 1.25−1.44 (24H, methylene),0.88 (3H, methyl). Found (calcd): C, 60.1 (59.69); H, 8.59 (8.65); N, 6.05 (6.33); S, 13.9(14.49). Compound **2** was water-soluble at pH > 8.5 and dissolved in acetone, DMF, and DMSO at 2.5 mM and room temperature.

Synthesis of Co(0) Nanoparticles without Capping Agents[58]. Cobalt chloride hexahydrate (238 mg, 1.0 mmol) dissolved in 15 mL ethylene glycol was mixed with an aqueous solution of NaOH (2 mmol in 20 mL). Hydrazine (1.6 g, 50 mmol) was slowly added to the resulting solution via syringe and the mixture was briefly sonicated and kept at 80 °C for 5 h, with intermittent vortexing. The formed particles were then separated from the supernatant by centrifugation (12 900 *g*, 5 min) and washed with excess ethanol, followed by centrifugation and repeated washing. The wash-outs were diluted 3-fold by deionized water and the pH of the resulting solution was measured to be 7.6, indicating that the excess hydrazine and sodium hydroxide was removed. The resulting particles were separated by centrifugation, dried under vacuum and stored in a desiccator in oxygen-free conditions, to prevent cobalt oxidation. For DLS measurements, the particles were dispersed in deionized water by brief sonication and then the number-average hydrodynamic diameter of the particles was measured within 1−2 min to be 7.1 ± 1.3 nm.

Synthesis of Co(0) Nanoparticles Modified by 9,10-trans-Epoxystearic Acid. Cobalt nanoparticles prepared without capping agents (20 mg) were suspended in a solution of 9,10-*trans*-epoxystearic acid (30 mg, 0.1 mmol, dissolved in 1.0 mL methanol) and briefly sonicated. To the suspension, 5 mL of deionized water was added and the suspension was vortexed. The particles were then separated from the reaction mixture by centrifugation at 12,900 *g*, suspended in 20 mL deionized water with brief sonication and the procedure of washing and separation was repeated

(57) Newman, J. W.; Hammock, B. D. *J. Chromatogr., A* **2001**, *925*, 223–240.
(58) Balela, M. D. L.; Lockman, Z.; Azizan, A.; Matsubara, E.; Amorsolo., A. V. *J.Phys. Sci.* **2008**, *9*, 1–11.

three times. The resulting Co(0) particles were water- and organic solvent-dispersible. The particles were characterized by DLS in water (pH 7), thermogravimetric analysis, and SQUID. The particles were found to have a number-average hydrodynamic diameter of 26 ± 11 nm, a saturation magnetization of ~25 emu/g of cobalt, and a fatty acid content of 22 wt %.

Synthesis of Co(0) Nanoparticles Modified by Oleic Acid. A solution of oleic acid (30 mg, 106 μmol, dissolved in 1.0 mL methanol) was suspended in 8 mL deionized water using brief sonication. To the suspension, a solution of cobalt chloride hexahydrate (238 mg, 1.0 mmol, dissolved in 2 mL water) was added, resulting in a pink-colored, opaque suspension, to which a solution of sodium borohydride (100 mg, 2.6 mmol in 3 mL water) was added under stirring. Foaming and formation of black-colored particles was observed. The reaction was allowed to proceed in a sealed flask for 16 h at room temperature with shaking. In a separate set of experiments, a freshly prepared solution of 2-mercaptoimidazole (150 mg, 1.5 mmol in 10 mL water) was added first, followed by addition of sodium borohydride (100 mg, 2.6 mmol in 3 mL water) to cobalt chloride hexahydrate and oleic acid suspension as above. The reaction was allowed to proceed identically to the one without 2-mercaptoimidazole. The particles were separated from the reaction mixture by centrifugation at 12 900 *g* and suspended in 50 mL of deionized water with brief sonication and the procedure of washing and separation was repeated three times. The resulting Co(0) particles were characterized by TEM, DLS in water (pH 7), thermogravimetric analysis and SQUID. After washing, the Co and S composition (wt%) of the cubical cobalt nanoparticles was: Co, 83.0; S, 0.75. No sulfur was detected in the particles prepared without 2-mercaptoimidazole. SQUID analysis of the cobalt NP modified with oleic acid yielded a saturation magnetization of approximately 25 emu/g of cobalt (S3).

Synthesis of Silver Nanoparticles in DMF. Silver nanoparticles were prepared by the reduction of $AgNO_3$ in *N*,*N*-dimethylformamide (DMF).[59] In a typical experiment, silver nitrate (2 g) and sodium borohydride (200 mg) were dissolved separately, each in 25 mL of DMF. Then, the borohydride solution was added dropwise into the silver nitrate solution in DMF. The color of the solution became black. The suspension was stirred and kept at 80 °C for 1 h to complete the reaction. At the end, a black precipitate was formed, which was centrifuged at 12 900 *g* and purified by washing with acetone, which was repeated three times to remove the excess DMF. The black precipitate was dried in a vacuum oven at 50 °C.

Synthesis of Silver Nanoparticles Modified by Oleic or 9,10-trans-Epoxystearic Acid. The black powder of silver particles prepared in DMF was dispersed in 15 mL of oleic acid (initial particle amount, 220 mg) or a solution of 9,10-*trans*-epoxystearic acid (50 mg acid 1 mL of DMF; initial particle amount, 30 mg), which was vortexed and vigorously shaken for 24 h at room temperature. The capped silver nanoparticles were centrifuged at 12 900 *g* and purified by washing with absolute ethanol. This process was repeated three times in order to remove the excess capping acid. Further removal of ethanol by vaporizing and drying in a vacuum oven gave a bright-black, dry powder of surface-modified silver nanoparticles. The particles capped with oleic and epoxystearic acid contained 24 and 16 wt % corresponding fatty acids, respectively.

Synthesis of Ag and Co Nanoparticles Modified by 2-Mercaptoimidazole and Oleic Acid Conjugate (**1**). The oleic-acid-capped Ag or Co particles (Co particles were prepared with the use of 2-mercaptoimidazole, see above) were further modified by conjugating 2-mercaptoimidazole with oleic acid on the particle surface using the thiol−ene reaction. Namely, 25 mg of particles modified with oleic acid were suspended in 2 mL of dry methanol with brief sonication, a solution of 2-mercaptoimidazole (4 mg, 40 μmol) and benzophenone (2 mg, 11 μmol) in 2 mL dry methanol was added, and the mixture was deaerated and placed in a glass vial, which was subsequently sealed and irradiated using a UV−vis 5000EC flood lamp (spectral output, 300−500 nm; maximum intensity, 250 mW/cm^2 at 365 nm; Dymax Corp, Torrington, CT) for 10 min. The resulting opaque suspension was equilibrated at ambient temperature, vacuum-evaporated, and resuspended in methanol (20 mL), following which the particles were separated by centrifugation (12 900 *g*, 5 min). The procedure of washing with methanol was repeated three times and the particles were vacuum-dried and kept at 4 °C prior to the use. The particles were visualized by TEM (S4). Silver particles modified with conjugate (1) (designated Silver NP-(**1**)) appeared to be aggregates of spherical particles of ~10 nm diameter, with the aggregate size of approximately 200 nm (S4), whereas modified Co particles (designated Cobalt NP-(**1**)) were cubical or octahedral, with an average size of ~100 nm (S5). These observations were corroborated by DLS measurements in water (pH adjusted to 7), yielding number-average hydrodynamic diameters of 190 and 130 nm for Silver NP-(**1**) and Cobalt NP-(**1**), respectively. TGA yielded the contents of Ag and Co to be 77 and 80 wt % in Silver NP-(**1**) and Cobalt NP-(**1**), respectively. SQUID measurements yielded a saturation magnetization of Cobalt NP-(**1**) to be 6.7 emu/g of cobalt (S3). Elemental analysis found, for silver NP-(**1**): C, 15.2; H, 2.51; Ag, 76.9; N, 1.68; S, 1.04; found, for cobalt NP-(**1**): C, 13.4; H, 2.31; Co, 77.4; N, 2.44; S, 2.95.

Modification of Ag or Co Nanoparticles with Epoxystearic and 4(5)-Imidazoledithiocarboxylic Acids Conjugate (**2**). The silver or cobalt NPs capped with 9,10-*trans*-epoxystearic acid (25 mg) were suspended in a solution of 4(5)-imidazoledithiocarboxylic acid (14 mg, 0.1 mmol, dissolved in 1.0 mL DMF) and the resulting suspension was kept at 70 °C for 8 h with intermittent vortexing. The resulting particles were separated by centrifugation (12 900 *g*, 5 min), diluted with 20 mL ethanol, briefly sonicated, and again separated by centrifugation. The procedure was repeated three times. The resulting particles were dried under vacuum and characterized by TGA, TEM (S6), and elemental analysis. SQUID measurements yielded a saturation magnetization of Cobalt NP-(**2**) to be approximately 2.0 emu/g of cobalt (S3). TGA measured the contents of Ag and Co to be 82 and 79 wt % in silver NP-(**2**) and cobalt NP-(**2**), respectively. Elemental analysis found, for Silver NP-(**2**): C, 11.8; H, 1.58; Ag, 81.0; N, 1.18; S, 2.69; found, for Cobalt NP-(**2**): C, 13.1; H, 1.91; Co, 78.7; N, 1.43; S, 3.11.

Complexes of Ligands and Nanoparticles with Co^{2+}. Complexes of ligands and nanoparticles with Co^{2+} were prepared by suspending the corresponding species in deionized water at 3−4 mg/mL concentration and adding an aqueous solution of cobalt(II) chloride hexahydrate (5 mL) resulting in a cobalt concentration that was equimolar to the corresponding ligand. The resulting suspension was separated by centrifugation (12 900 *g*, 20 min) and the remaining blue paste or solids were lyophilized and stored at −20 °C prior to the use.

Characterization Methods. *NMR Spectroscopy and Kinetics of Paraoxon Hydrolysis.* ^{1}H and ^{31}P NMR spectra were collected at 25 ± 0.5 °C using a Bruker Avance-400 spectrometer operating at 400.01 and 161.98 MHz, respectively. ^{1}H NMR spectra

(59) Chen, M.; Ding, W. H.; Kong, Y.; Diao, G. W. *Langmuir* **2008**, *24*, 3471–3478.

were measured with solutions of ligands in deuterated solvents. The kinetics of paraoxon degradation were determined using ^{31}P NMR. Spectra (1500 scans for cobalt chloride solutions and 64 scans for all other samples) were recorded using an 85% phosphoric acid solution in D_2O as an external reference (0 ppm). The reaction milieu consisted of 50 mM HEPES buffer in D_2O to keep the solution pH constant at 9. The reaction time was taken to be the midpoint of the acquisition period. For kinetic measurements with nonmagnetic materials, samples of 2−3 mg/mL of ligand or silver nanoparticle-based suspension in HEPES/D_2O solution (50 mM, pH 9.0) and paraoxon solution in acetonitrile (50 mM) were prepared. Basic pH accelerated the spontaneous hydrolysis of paraoxon to acceptable levels versus neutral pH, and buffering allowed for maintenance of constant reaction rate up to high degrees of conversion. Acetonitrile was added to improve the miscibility of paraoxon (aqueous solubility at 20 °C, up to 3.6 mg/mL)[60] and aqueous buffer as well as to act as a convenient reactant diluent that did not trigger the reaction prior to contact with the aqueous phase. At $t = 0$, 630 μL of ligand or nonmagnetic particle suspension and 70 μL of paraoxon solution were mixed by vortexing and placed into an NMR tube for kinetic measurements. Paramagnetic cobalt NP-based suspensions (3 mg/mL) in HEPES/D_2O buffer (50 mM, pH 9.0) were prepared as a 5 mL stock sample, which was mixed with 556 μL of paraoxon in acetonitrile at $t = 0$, resulting in the initial paraoxon concentration of 5 mM. The final suspension was kept at room temperature while shaking. At given time intervals, the suspension was centrifuged (6,500 *g*, 5 min), and the top clear solution (0.7 mL) was carefully withdrawn by a pipet and placed into an NMR tube. The solution was placed back into the suspension immediately after each NMR measurement. The degree of paraoxon conversion was expressed as[9]

$$F_t = \Sigma I_p/(\Sigma I_r + \Sigma I_p) \quad (1)$$

where ΣI_r and ΣI_p are the sums of the integrations of the signals corresponding to the reactant (paraoxon, −6.11 ppm) and the products (diethyl phosphate, 1.22 ppm, and diethyl phosphate-HEPES adduct[61]), respectively (S7). The observed rate constant, k_{obs}, is found from the slope of the $\ln(1 - F_t)$ vs t plot:

$$\ln(1 - F_t) = -k_{obs}t \quad (2)$$

Transmission Electron Microscopy (*TEM*). TEM was performed on a JEOL 200-CX transmission electron microscope. Samples were prepared by placing drops of the nanoparticle dispersion on lacey carbon-coated 200 Mesh copper grids (Structure Probe, Inc.) and imaged at an accelerating voltage of 200 kV.

Fourier Transform Infrared Spectroscopy (*FTIR*). FTIR spectroscopy was performed on a NEXUS 870 FTIR spectrometer (Thermo Nicolet Inc.). Spectra were recorded over the wavenumber range between 4000 and 400 cm^{-1} at a resolution of 2 cm^{-1} and are reported as the average of 64 spectral scans. All samples were dried under a vacuum to constant weight, ground and blended with KBr, and pressed to form the pellets used in the measurements.

Superconducting Quantum Interference Device (*SQUID*) experiments were conducted using a magnetic property measurement system model MPMS-5S (Quantum Design) to determine the magnetization of the particles in an applied magnetic field. All SQUID measurements were performed at 300 K over a 0 to +50 kOe range on dried particles weighing 5−7 mg.

ζ-Potential Measurements. All ζ-potential measurements were performed using a Brookhaven ZetaPALS ζ-potential analyzer (Brookhaven Instruments Corporation). The Smoluchowski equation was used to calculate the ζ-potential from the electrophoretic mobility. The reported ζ-potential values are an average of 5 measurements, each of which was obtained more than 25 electrode cycles. The particles were dispersed in 5 mM KCl aqueous solution at approximately 0.05 wt % concentration and the pH of the nanoparticle suspensions was adjusted by adding 1 M HCl or NaOH aqueous solutions.

Dynamic Light Scattering (*DLS*). Dynamic light scattering (DLS) experiments were performed with a Brookhaven BI-200SM light scattering system (Brookhaven Instruments Corporation) at a measurement angle of 90°. Number-average particle size distributions were obtained using the built-in software and the reported particle mean hydrodynamic diameters are the average of five measurements, each conducted for 3 min. All samples dispersed in aqueous 10 mM KCl (pH adjusted by 1 M NaOH or HCl) were filtered with a 0.45 μm syringe filter prior to the DLS tests.

Molecular weight and other structural parameters of ligands and nanoparticles were calculated using ChemBioDraw Ultra version 12.0 software (CambridgeSoft Co.).

Results and Discussion

Ligand and Particle Syntheses and Characterization. As stated in the Introduction, we wished to develop a straightforward synthetic route toward fatty acids that are modified by a reactive moiety capable of chelating with transition metal ions and accelerating the hydrolysis of organophosphorous esters. Neither 9-((1H-imidazol-2-yl)-thio)octadecanoic acid (**1**) nor 9-((1H-imidazole-5-carbonothioyl) thio)-8-hydroxyoctadecanoic acid (**2**) and their syntheses via the thiol−ene reaction of oleic acid and 2-mercaptoimidazole (Figure 1), and *trans*-9,10-epoxystearic and 4(5)-imidazoledithiocarboxylic acids (Figure 2), respectively, have been previously reported. The one-step synthetic routes described herein are facile and produce acceptable yields, limited only by the product purification processes, as is common for fine fatty acid derivatives. The targeted fatty acid derivatives **1** and **2** are multidentate ligands with thiol, amine, and carboxylic groups capable of complexation with metal ions. Thiol sulfur, dithiocarboxylic moieties and imidazole nitrogens possess inherently stronger coordination and chelation capability with metals than do carboxyl groups.[62−65] Therefore, in order to maintain the NP complexation by fatty acids through metal-carboxyl binding, we synthesized oleic acid- or epoxystearic acid-modified particles, which were subsequently modified by 2-mercaptoimidazole or (4)5-imidazoledithiocarboxylic acid (Figures 1 and 2). If

(60) Bowman, B. T.; Sans, W. W. *J. Environ. Sci. Health* **1979**, *B14*, 625–634.
(61) Gäba, J.; John, H.; Melzer, M.; Blum, M.-M. J. Chromatogt., B **2010**, in press.
(62) Ceretti Mazza, M. T.; De Cicco, L.; De Rosa, G.; Caramazza, R. J. *Biol. Res.−Boll. Soc. It. Biol. Sper*. **1996**, *72*, 79–86.
(63) Sakurai, H. *Transition Met. Chem*. **1977**, *2*, 103–106.
(64) Ahrland, S.; Chatt, J.; Davies, N. R. *Q. Rev. Chem. Soc*. **1958**, *12*, 265–276.
(65) Watt, J.; Cheong, S.; Toney, M. F.; Ingham, B.; Cookson, J.; Bishop, P. T.; Tilley, R. D. *ACS Nano* **2010**, *4*, 396–402.

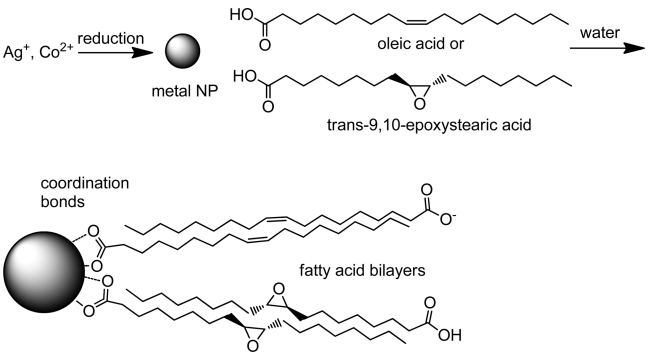

Figure 3. Schematic of nanoparticle synthesis by metal ion reduction followed by complexation with fatty acids.

we were to bind multidentate compounds **1** and **2** to cobalt or silver NP directly, the metal−thiol or metal-imidazole chelation would have been more likely than metal−carboxyl. The synthetic routes toward fatty-acid-chelated NP in the present study are shown in Figure 3.

Notably, in our synthetic route, the nanoparticles were first prepared by reduction of the corresponding cobalt or silver salts by sodium borohydride, purified, and then complexed with fatty acids. Reduction of silver and cobalt salts by sodium borohydride in the presence of oxygen is well-known[55,65−67]

$$AgNO_3 + NaBH_4 \rightarrow Ag + 0.5H_2 + 0.5B_2H_6 + NaNO_3$$

$$2CoCl_2 + 4NaBH_4 + 9H_2O \rightarrow Co_2B + 4NaCl + 12.5H_2 + 3B(OH)_3$$

$$4Co_2B + 3O_2 \rightarrow 8Co + 2B_2O_3$$

In the case of Co(II), when the mixture is exposed to oxygen, a sacrificial reaction takes place whereby boron is oxidized while cobalt is reduced, resulting in the conversion of Co_2B to Co(metal).[67]

Interestingly, the structures of the Co NPs prepared with and without 2-mercaptoimidazole appeared to be quite different (Figure.4). Particles prepared with oleic acid as the only capping agent aggregated into ∼200 nm clusters composed of ∼10 nm spherical primary particles (Figure.4a), whereas the particles prepared in the presence of both 2-mercaptoimidazole and oleic acid were cubical or octahedral in shape, with one side of the cube sized ∼50 nm (Figure.4b). Although the formation of cubical particles in the presence of both mercaptoimidazole and oleic acid is a novel observation of the present study, it has been reported previously that simultaneous presence of several agents strongly binding to the nanocrystal surface such as oleic acid, trioctylphosphine oxide, and others affects the shape of the cobalt crystals.[56]

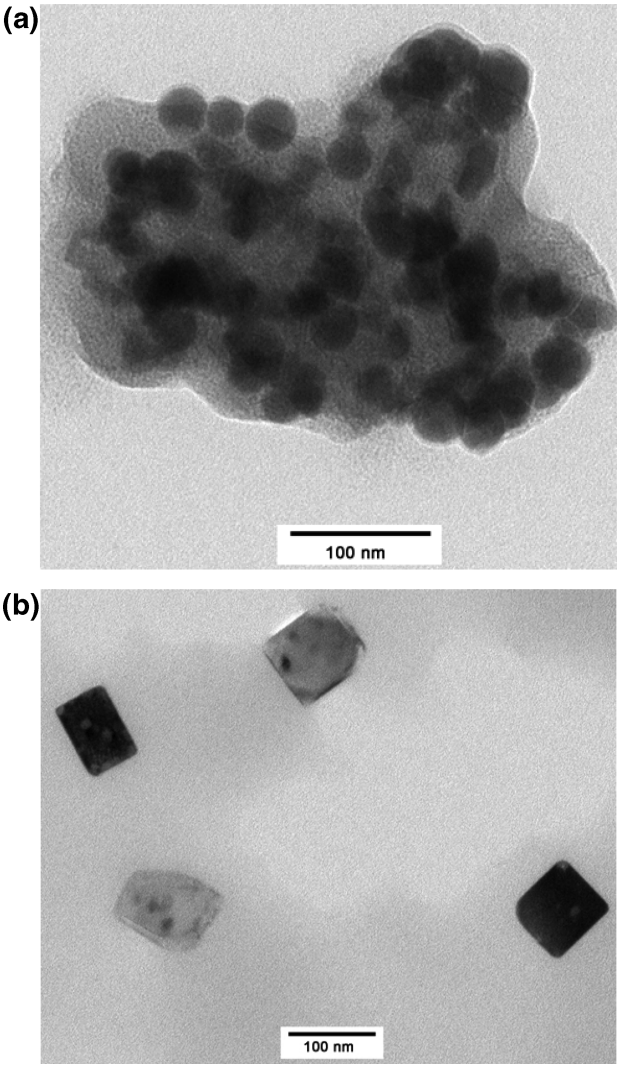

Figure 4. (a) TEM image of Co nanoparticles synthesized by reduction of cobalt(II) chloride hexahydrate by sodium borohydride in the presence of oleic acid only. (b) TEM image of Co(0) nanoparticles synthesized by reduction of cobalt(II) chloride hexahydrate by sodium borohydride in the presence of 2-mercaptoimidazole and oleic acid. For synthesis details, see Experimental Section.

It has been argued[68] that the reduction of silver sulfate by borohydride directly in the presence of oleic acid results in the binding of the silver nanoparticle surface to the oleic acid through the double bond. We believe that in our synthesis (Figure 3), because the reduction was completed prior to the contact of fatty acids with the resulting NP, the adsorption of the fatty acids on the Ag or Co surface is through the carboxylate groups. Small angle neutron scattering, magnetization analysis, and other techniques have been previously used to demonstrate that metal or metal oxide nanoparticles modified with excess monocarboxylic acids form double layers of the acids on the particle surface in water, which helps to stabilize the particles colloidally.[69−73] The ζ-potential measured in 5 mM KCl at pH 7.0 was −22 ± 3 mV

(66) Glavee, G. N.; Klabunde, K. J.; Sorensen, C. M.; Hadjipanayis, G. C. *Langmuir* **1993**, *9*, 162–169.
(67) Glavee, G. N.; Klabunde, K. J.; Sorensen, C. M.; Hadjipanayis, G. C. *Langmuir* **1992**, *8*, 771–773.
(68) Bala, T.; Swami, A.; Prasad, B. L. V.; Sastry, M. *J. Colloid Interface Sci.* **2005**, *283*, 422–431.
(69) Shen, L.; Laibinis, P. E.; Hatton, T. A. *Langmuir* **1999**, *15*, 447–453.
(70) Shen, L.; Stachowiak, A.; Fateen, S.-E. K.; Laibinis, P. E.; Hatton, T. A. *Langmuir* **2001**, *17*(2), 288–299.

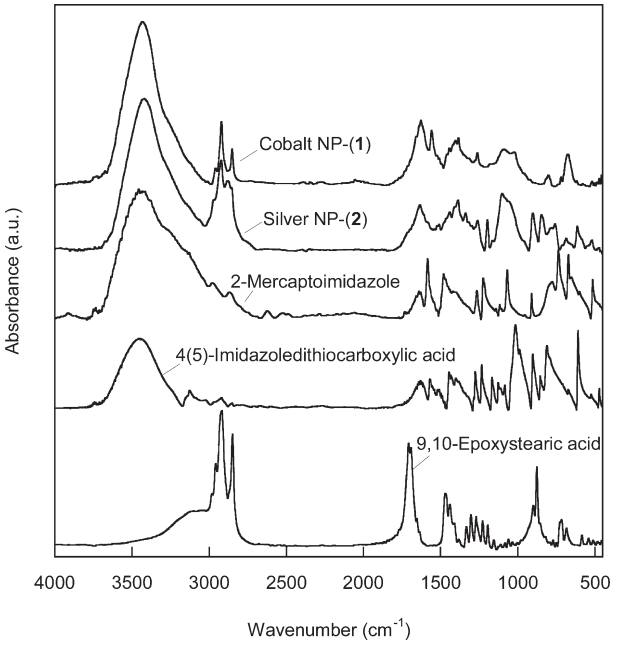

Figure 5. FTIR spectra of cobalt NP-(**1**), silver NP-(**2**), and their representative precursors: 2-mercaptoimidazole, 4(5)-imidazoledithiocarboxylic acid, and *trans*-9,10- epoxystearic acid.

(silver-epoxystearic acid NP) and -28 ± 2 mV (cobalt-oleic acid NP), indicating that the particles are stabilized by the negative charge of the carboxylate groups exposed to the outer layer of the water-bilayer interface.

Modification of particles capped by oleic or epoxystearic acid by the thiol−ene reaction with mercaptoimidazole (Figure.1) or condensation with imidazoledithiocarboxylic acid (Figure.2), respectively, was evident from the spectroscopic data (Figure.5). Thus, FTIR spectra of the silver and cobalt NP-(**1**) and NP-(**2**) featured two strong bands at about 2920 and 2850 cm^{-1}, typical of the antisymmetric and symmetric CH stretching vibrations, respectively, because of the fatty acid components.[74] The spectra also showed bands characteristic of vibrations of the imidazole ring (amidine bands around 1640−1650 cm^{-1}), and C−C−S stretching bands at 686 cm^{-1} (cobalt NP-(**1**)). The strong band characteristic of the free carboxylate group at 1710 cm^{-1} in the fatty acid as well as free conjugates **1** and **2** (not shown) was present only as a shoulder of a broader signal centered in the 1640 cm^{-1} area in the NP spectra. Overall, the FTIR spectra support the structure wherein imidazole-containing conjugates are adsorbed onto the NP metal surfaces via carboxylate-metal complexation.

Further quantitative information on the ratio of metal to organic ligands comes from the TGA and elemental analysis (see the Experimental Section). On the basis of these analyses, we estimate that the average NP modified with conjugate **1** contained approximately one molecule of **1** per 25 silver and 27 cobalt atoms, respectively, whereas NP modified with conjugate **2** contained approximately one molecule of **2** per 18 silver and 27 cobalt atoms, respectively. On the basis of the elemental analysis, and assuming the average diameter of a single particle to be 10 nm, we estimate that the area occupied by a single ligand on Ag and Co nanoparticle surface in our experiments is in the range 0.08−0.15 nm^2. For comparison, the mean molecular area occupied by a single oleic acid molecule is about 0.42 nm^2/molecule.[75,76] Given that the ligands **1** and **2** are significantly larger than the oleic acid molecule because of the attachment of the imidazole moieties, we can conclude that the ligands were attached to the NPs in multilayers. The calculations were performed assuming conjugate structures on the NP surface to be of those depicted in Figures 1 and 2.

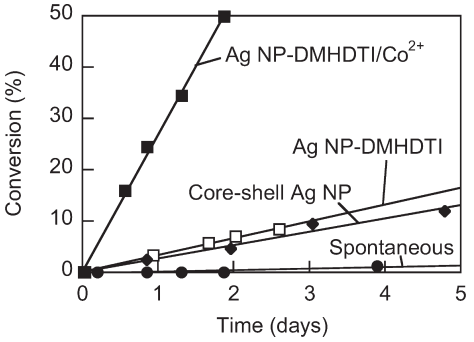

Figure 6. Representative kinetics of paraoxon decomposition, both spontaneous and catalyzed by silver NP-(**1**) and the same nanoparticles complexed with Co^{2+}.

Ligand and Nanoparticle Performance in Organophosphate Hydrolysis. We studied the performance of the ligands attached to the nanoparticles in the hydrolysis of the organophosphate insecticide, paraoxon. The kinetics of the insecticide hydrolysis was studied in aqueous solutions containing 10% acetonitrile. The pH was kept constant at 9.0 throughout the study. The basic pH accelerated the spontaneous hydrolysis of paraoxon to acceptable levels versus neutral pH, and buffering allowed for maintenance of constant reaction rate up to high degrees of conversion. The reaction was followed by ^{31}P NMR as described in the Experimental Section and typical kinetics data are shown in Figure 6.

When the kinetics results were expressed in terms of eq 2, the curve fits were linear ($R^2 > 0.98$ in all cases), indicating a pseudo-first-order reaction order. The observed rate constants afforded calculation of the reaction half-life ($\tau_{1/2} = \ln(2)/k_{obs}$) and the apparent second-order rate constant $k'' = k_{obs}/C_{cat}$, where C_{cat} is the initial effective molar concentration of the catalytic groups. The results of all kinetic measurements are collected in Table 1. As is seen, weakly nucleophilic 2-mercaptoimidazole

(71) Avdeev, M. V.; Aksenov, V. L.; Balasoiu, M.; Garamus, V. M.; Schreyer, A.; Toeroek, Gy.; Rosta, L.; Bica, D.; Vekas, L. *J. Colloid Interface Sci.* **2006**, *295*, 100–107.
(72) Yanga, K.; Penga, H.; Wen, Y.; Li, N. *Appl. Surf. Sci.* **2010**, *256*, 3093–3097.
(73) Avdeev, M. V.; Mucha, B.; Lamszus, K.; Vékás, L.; Garamus, V. M.; Feoktystov, A. V.; Marinica, O.; Turcu, R.; Willumeit, R. *Langmuir* **2010**, *26*, 8503–8509.
(74) Kimura, F.; Umemura, J.; Takenaka, T. *Langmuir* **1986**, *2*, 96–101.
(75) Lundgren, S. M.; Persson, K.; Mueller, G.; Kronberg, B.; Clarke, J.; Chtaib, M.; Claesson, P. M. *Langmuir* **2007**, *23*, 10598–10602.
(76) Pichon, B. P.; Demortiere, A.; Pauly, M.; Mougin, K.; Derory, A.; Begin-Colin, S. *J. Phys. Chem. C* **2010**, *114*, 9041–9048.

Table 1. Half-Life ($\tau_{1/2}$) and Apparent Second-Order Rate Constant (k'') of Paraoxon Hydrolysis in the Presence of Ligands and Nanoparticles of the Present Study at pH 9.0

system[a]	half-life, $\tau_{1/2}$ (days)	second-order rate constant, k'' ($\times 10^4$ M^{-1} s^{-1})[b]
spontaneous hydrolysis	> 140	
2-mercaptoimidazole	35	1.2
stoichiometric complex 2-mercaptoimidazole/Co^{2+}	2.6	16
4(5)-imidazoledithiocarboxylic acid	11	3.6
stoichiometric complex 4(5)-imidazoledithiocarboxylic acid/Co^{2+}	6.6	6.1
silver NP-(**1**)	20	4.9
silver NP-(**2**)	24	1.5
stoichiometric complex Silver NP-(**1**)/Co^{2+}	1.9	53
Co^{2+}	21	0.30
cobalt NP-(**1**)[c]	5.8	2.1
cobalt NP-(**2**)	32	0.38
stoichiometric complex Cobalt NP-(**2**)/Co^{2+}	2.3	18

[a] Each system comprised 10 vol % acetonitrile solution in 50 mM HEPES/D_2O (pD 9.0). [b] Apparent second-order rate constants were calculated from $k'' = r_o/C_sC_{cat}$, where $r_o = k_{obs}C_s$ is the initial reaction rate, C_s and C_{cat} are initial effective concentrations of the substrate (paraoxon) and catalyst, respectively. The C_{cat} values were calculated as effective molar concentrations of the catalytic groups. [c] Synthesized in the presence of 2-mercaptoimidazole and oleic acid (see Experimental Section).

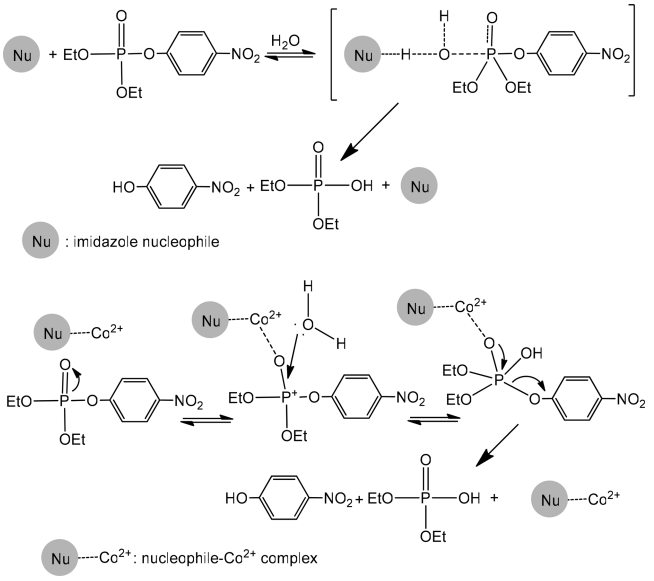

Figure 7. Schematic of paraoxon hydrolysis acceleration by nucleophile such as imidazole and its derivatives and nucleophile-Co^{2+} complex.

afforded only approximately 4-fold faster paraoxon degradation compared to the spontaneous hydrolysis, but 4(5)-imidazoledithiocarboxylic acid was approximately 12-fold more active because of its higher nucleophilicity. Cobalt chloride solution per se was not particularly reactive. However, stoichiometric complexation of either of 2-mercaptoimidazole or 4(5)-imidazoledithiocarboxylic acid with cobalt ions resulted in a significant, up to 13-fold acceleration of the paraoxon hydrolysis. The same synergistic effect of the presence of both imidazole-containing ligands and cobalt ions was observed with nanoparticles modified with conjugates **1** and **2**, where ligand complexation with Co^{2+} resulted in 10- to almost 50-fold hydrolysis acceleration. Mechanistically, such a phenomenon can be explained[49] by the ability of the Co^{2+} or Co^{2+}-imidazole ligand to coordinate the oxonate oxygen, withdrawing electron density from the phosphorus atom and generating a more reactive electrophile capable of efficient hydrolysis even by moderately nucleophilic ligands such as imidazole. Schematics of both imidazole ligand- and ligand-Co^{2+} mechanisms of hydrolysis are presented in Figure 7. Similarly, acceleration of the paraoxon hydrolysis has been observed with vinylimidazole-containing polymers chelated ("molecularly imprinted") with Co^{2+}.[77] An analogy between such an active imidazole-Co^{2+} complex and the active site of phosphotriesterase with Co^{2+} ions coordinated to histidine[78,79] can be seen. To the best of our knowledge, ours is the first encounter of such a "biomimetic" catalytic activity of nanoparticles complexed with metal ions.

Conclusions

For the first time, we described a facile synthesis of imidazole-containing ligands that are conjugated to fatty acid chains via a thiol−ene reaction between oleic acid and 2-mercaptoimidazole and a condensation between (4)5-imidazoledithiocarboxylic and 9,10-epoxystearic acids. To obtain the ligands bound to the metal surface by the carboxyl groups, we first synthesized NPs of Ag(0) and Co(0) by conventional reduction of corresponding salts by sodium borohydride. Then the adsorbed oleic or 9,10-epoxystearic acids were further modified by 2-mercaptoimidazole and (4)5-imidazoledithiocarboxylic acid, respectively. As a variation of the "fatty acid adsorption first" synthesis, we were able to obtain Co(0)-based NPs by reduction of Co^{2+} in the presence of both the fatty acid and 2-mercaptoimidazole, which unexpectedly resulted in the NPs of cubical or octahedral shape, as opposed to spherical particles formed in the presence of oleic acid only. The thio- and dithio- imidazole ligands and NPs demonstrated significant, albeit moderate activity in catalyzing esterolysis of paraoxon, but their complexes with Co^{2+} were 10- to 50-fold more reactive. The uncovered synergistic effect of the Co^{2+} (but not Co(0) in the nanoparticle core) and imidazole derivatives mimics that of the metal-histidine moieties in the active site of enzymes in that the metal−ligand complex is far more reactive than the ligand itself. The described NPs were readily recovered from the reaction medium by filtering or centrifugation and in that sense were advantageous as catalysts over their organic ligands without the metal core. In addition, the metal cores resulted in intense coloring of the particles, which can be exploited for particle detection in our ongoing studies.

(77) Yamazaki, T.; Yilmaz, E.; Mosbach, K.; Sode, K. *Anal. Chim. Acta* **2001**, *435*, 209–214.
(78) Omburo, G. A.; Kuo, J. M.; Mullins, L. S.; Raushel, F. M. *J. Biol. Chem.* **1992**, *267*, 13278–13283.
(79) Kuo, S.J. M.; Raushel, F. M. *Biochemistry* **1994**, *33*, 4265–4272.

Acknowledgment. This work was sponsored by the Defense Threat Reduction Agency grant HDTR1-09-1-0012 and supported via the Department of the Army, U.S. Army Research Office, under Grant W911NF-07-1-0139. Any opinions, findings, conclusions, and recommendations expressed in this paper are those of the authors and do not necessarily reflect the view of the U.S. Army Research Office. The authors are grateful to Dr. Takuya Harada for help with TEM and SQUID measurements.

Supporting Information Available: ^{1}H NMR spectra of functional ligands, TEM images of modified Ag and Co nanoparticles, SQUID particle characterization, and ^{31}P NMR of paraoxon degradation (PDF). This material is available free of charge via the Internet at http://pubs.acs.org.